# The Role of *Nexmifb* in Regulating Spinal Motor Neuron Development through *Efna5b* in Zebrafish

**Mei Sun[1,2], Jingwen Ma[1,2], Zirui Zhou[1,2], Lingling Li[1,3], Youjia Wu[1], Guihai Suo[1,*], Yuqin Zheng[1,*]**

[1] Department of Pediatrics, Affiliated Hospital of Nantong University, Nantong, China
[2] Nantong University, Nantong, China
[3] Nantong Second People's Hospital, Nantong, China

***Correspondence:** Yuqin Zheng and Guihai Suo, Department of Pediatrics, Affiliated Hospital of Nantong University, Nantong 226001, China.
E-Mails: 403006970@qq.com and 27456469@qq.com

**Abstract**

**Objective:** To confirm the role of *nexmifb* in the development of spinal motor neuron in zebrafish and explore its molecular mechanism.

**Methods:** Detect the localization and expression of *nexmifb* in zebrafish by whole-mount *in situ* hybridization. Establish a *nexmifb* knockdown model by morpholino technology. Measure the body length of zebrafish at 72 hours post-fertilization (hpf) in both the control group and the *nexmifb* knockdown group. Observe the morphology of spinal motor neurons at the 72 hpf laser confocal microscopy in both groups. Motor neuron apoptosis was assessed using the terminal deoxynucleotidyl transferase mediated dUTP nick end labeling (TUNEL) assay kit in both groups. Perform the transcriptome sequencing on embryos from both groups at 72 hpf, then identify the interest gene of *efna5b*. Observe the rescue effect of *efna5b* on spinal motor neurons in the *nexmifb* knockdown group.

**Results:** *nexmifb* was primarily expressed in the brain and spinal cord of zebrafish. Knockdown of *nexmifb* resulted in shortened body length, loss of spinal motor neurons, reduced caudal primary motor neurons (Caps) length, and decreased branching number per mm of Cap. Overexpression of *efna5b* partially rescued these abnormal phenotypes.

**Conclusion:** *nexmifb* regulates spinal motor neuron development by downregulating *efna5b*.

**Keywords:** *nexmifb*; motor neuron; *efna5b*; zebrafish

*NEXMIF* (also called *KIDLIA*, *KIAA2022*, or *XPN*) is a novel gene localized in Xq13.2. It was first reported in two males with intellectual disability in 2004[1]. So far, little is known about *NEXMIF*. It has been reported that *NEXMIF* is associated with multisystem diseases, for example, patients with *NEXMIF* mutations present with X-linked mental retardation[1]. RNA-Seq indicates that *NEXMIF* expression is significantly down-regulated in Down syndrome patients with atrial septal defect and/or ventricular septal defect compared with patients without these defects[2]. *Nexmif* knockout mice exhibit smaller islets and glucose intolerance compared with the control

**Received:** 24 November 2025; **Accepted:** 31 December 2025
**DOI:** 10.2738/TNN.2026.0003

group[3]. However, research on *NEXMIF* remains primarily focused on its effects on the central nervous system (CNS). This may be attributed to its high expression in the CNS especially in the developing brain[4]. In humans, *NEXMIF* mutations are not only associated with X-linked mental retardation but also different types of epilepsy, autism spectrum disorder, and other CNS-related diseases[1,5–7]. In animal models, *NEXMIF* is important in regulating neurite morphological development, cell migration, and cell-matrix adhesion, and maintaining normal synaptic function. For example, loss of *NEXMIF* altered the migration of layer II/III cortical neurons in mice, reduced dendrite growth, and disturbed apical dendrite projection. Knockdown of *Nexmif* in cultured rat hippocampal neurons affected axonal development[8], and knockdown in PC12 cells enhanced N-cadherin and β1-integrin-mediated cell-cell and cell-matrix adhesion, thereby inhibiting cell migration[9]. Loss of *NEXMIF* in mice decreased synapse density, spine density, and the expression of synaptic-related proteins[10]. These results indicate that *NEXMIF* plays an important role in CNS development.

Zebrafish is a powerful model organism for studying development and regeneration[11]. There are two kinds of spinal motor neurons in zebrafish named primary motor neurons (PMNs) and secondary motor neurons[12,13]. PMNs can be further divided into three groups in each spinal hemisegment according to their somata position and specific axonal projection pathway, they are caudal PMNs (CaPs), middle PMNs (MiPs), and rostral PMNs (RoPs)[13,14]. Although the somata of the three kinds of PMNs are localized at different positions in the spinal cord, their axons travel to the myoseptum via a common exit point and project their axons to innervate the corresponding muscles[15]. The three groups of PMNs are readily identifiable; therefore, they have become excellent cell systems for elucidating motor axon guidance mechanisms *in vivo*[16].

In zebrafish, *nexmif* has two paralogs, *nexmifa* and *nexmifb* (ENSDARG00000029296). Our previous study has indicated that *nexmifa* can regulate spinal motor neuron morphogenesis[17]. In this study, we established the *nexmifb* knockdown model (*nexmifb* morphant) by injecting *nexmifb* translation-blocking morpholinos (MOs) into zebrafish embryos and performed RNA sequencing (RNA-Seq) to explore the function and mechanism of *nexmifb* in spinal motor neuron development.

## Materials and methods

### Zebrafish husbandry and strain

Wild-type and Tg (*mnx1*: GFP)$^{ml2}$ zebrafish were maintained in the Zebrafish Center at Nantong University under guidelines outlined in previous studies[17].

### Whole mount in situ hybridization (WISH)

WISH was performed according to our previous study[19]. cDNA fragments of *nexmifb* and *efna5b* from zebrafish embryos were amplified using their specific primers (*nexmifb*-F: 5′-AATTGCCCGACTCTTACCCA-3′, *nexmifb*-R: 5′-TCTCAGGGGTGTGATTGCAT-3′, *efna5b*-F: 5′-TCCAGCCTCCATGATCACA-3′, *efna5b*-R: 5′-TTTGTTACGGGAAGGCAGAC-3′). Digoxigenin-labeled sense and antisense probes were synthesized using a linearized pGEM-Teasy vector subcloned with the above six fragments by *in vitro* transcription using the DIG-RNA Labeling Kit (Roche, Basel, Switzerland). Pictures were taken with an Olympus DP70 camera on an Olympus stereomicroscope MVX10.

### Quantitative RT-PCR

Tg(*mnx1*:GFP)$^{ml2}$ zebrafish embryos were collected at 72 hours post fertilization (hpf). Total RNA was extracted by TRIzol reagent (Invitrogen, Waltham, MA, United States) from zebrafish embryos. cDNA was synthesized using Transcriptor First Strand cDNA Synthesis Kit (Fermentas, Waltham, MA, United States) and stored at –20 °C. Quantitative RT-PCR (qRT-PCR) was carried out using the corresponding primers: *nexmifb*-F: 5′-TCCCAGGCAGGAGGTTTCTTCTAC-3′, *nexmifb*-R: 5′-GGGCGGCAGTGTGTATGATGTC-3′, *nexmifa*-F: 5′-GATGATGACTGGTGCCCGAAGAAG-3′, *nexmifa*-R: 5′-CAGACGACAGCAGGTGATGGTTC-3′, *efna5b*-F: 5′-GCAGGCGGAGATGATCGTGTTC-3′, *efna5b*-R: 5′-TTCGGTTCCAGAAGACAGCATATCG-3′, *ef-1α*-F: 5′-CTTCAACGCTCAGGTCATCA-3′, *ef-1α*-R: 5′-CGGTCGATCTTCTCCTTGAG-3′.

### MOs and microinjection

We synthesized *nexmifb* translation-blocking MOs and standard control MOs using Gene Tools. Diluted them to 0.3 mM, and injected into embryos to

establish *nexmifb* knockdown and control zebrafish embryos. The embryos were cultured in E3 medium at 28.5 °C for the following experiment. The sequence of *nexmifb* MOs was 5′-AATCTGAATGTGGTCT-TCCTTGGAA-3′. The sequence of standard MOs was 5′-CCTCTTACCTCAGTTACAATTTATA-3′. To perform rescue experiments, we generated *efna5b* mRNAs *in vitro*. The open reading frames of *efna5b* were amplified and cloned into the $PCS^{2+}$ vector. After linearization, the 5′-capped *efna5b* mRNAs were synthesized and purified *in vitro* using the mMESSAGE mMACHIN Kit (Ambion, Austin, Texas, United States) and RNeasy Mini Kit (Qiagen, Hilden, Germany). MOs and mRNAs were injected singly or combined into the yolk of one-cell stage embryos using borosilicate glass capillaries and a PV830 pneumatic pico pump (Sarasota, Florida, United States).

### Terminal deoxynucleotidyl transferase mediated dUTP nick end labeling (TUNEL) assay

Control and *nexmifb* morphants were collected at 72 hpf and fixed in 4% paraformaldehyde at room temperature for 2 h. After washing three times with PBS for 5 min each, 20 μg/mL proteinase K was added for 10 min to digest embryos, which were washed with PBS three times for 5 min each. The TUNEL assay was carried out using the TUNEL BrightRed Apoptosis Detection Kit (Vazyme, Nanjing, China).

### cDNA library preparation and RNA-Seq

Total RNA was extracted by TRIzol reagent from *nexmifb* morphants and control embryos at 72 hpf. RNA integrity and purity were calculated by NanoDRop 2000 (Thermo Fisher Scientific Inc., Waltham, MA, United States). RNA samples with OD260/280 1.8–2.2 and RNA Integrity Number ≥ 8.0 were used to construct the sequencing library. An Illumina NovaSeq 6000 platform, with 2 × 150-bp pair-end reads (Illumina, San Diego, CA, United States) was used to quantify and sequence the final cDNA libraries. Clean reads were obtained from the screening of raw reads. Download reference genome sequences and gene model annotation files from ENSEMBL. Hisat2 (v2.0.1) was used to index reference genome sequences. Finally, clean reads were aligned to the reference genome via the software Hisat2 (v2.0.1). Differential expression analysis was conducted with the DESeq2 (V1.6.3) Bioconductor package. The false discovery rate was controlled through Benjamini and Hochberg's approach by adjusting the resulting *P* value. Genes both with an adjusted *P* value < 0.05, and fold change value > 2 were confirmed as DEGs.

### Image acquisition and statistical analysis

Zebrafish embryos were anesthetized with tricaine (Sigma, Saint Louis, Missouri, United States) at 48 and 72 hpf, embedded in 0.8% low melting point agarose, and observed by Leica TCS-SP5 LSM confocal imaging. Statistical analysis was performed using SPSS version 21.0 software (SPSS, Armonk, NY, United States). Student's t-test or one-way analysis of variance was used to compare the data. $P < 0.05$ was considered statistically significant.

## Results

### Nexmifb is expressed in the spinal cord of zebrafish

To detect the expression of *nexmifb* in zebrafish, WISH

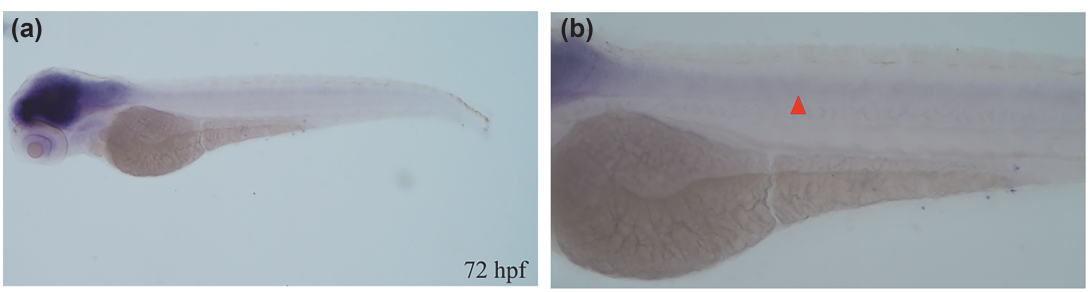


**Figure 1:** *nexmifb* expression in CNS ((a) WISH showed that nexmifb was mainly expressed in the brain and spinal cord (marked with red arrowheads); (b) Enlarged image of partial torso shown in (a)).

was performed at 72 hpf. The results showed *nexmifb* mRNA was mainly expressed in the brain and spinal cord (Figures 1(a) and 1(b)).

## Knockdown of nexmifa or nexmifb did not affect expression of the other paralog

In zebrafish, *nexmif* has two paralogs, *nexmifa* and *nexmifb*. We perform qRT-PCR to determine whether *nexmifa* or *nexmifb* knockdown affected of the other paralog. The result showed that there was no significant difference in the expression level of *nexmifb* mRNA between control and *nexmifa* morphants at 72 hpf (Figure 2(a)). There was also no significant difference in the expression of *nexmifa* between the control and *nexmifb* morphants (Figure 2(b)), which indicated that knockdown of *nexmifa* or *nexmifb* did not affect expression of the other paralog.

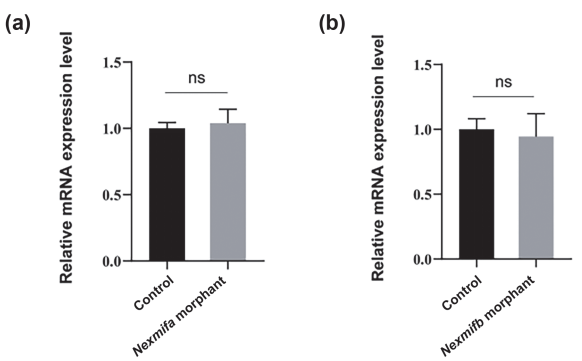


**Figure 2:** Detect whether knockdown of *nexmifb* or *nexmifa* affected expression of the other paralog ((a) Expression of nexmifb between control and *nexmifa* morphants, as shown by qRTPCR; (b) Expression of *nexmifa* between control and *nexmifb* morphants, as shown by qRT-PCR; ns: non-significant).

## Knockdown of nexmifb affected the body length of zebrafish

We found that no significant malformations were observed in the external appearance of *nexmifb* knockdown zebrafish embryos. However, at 72 hpf, the body length of zebrafish in the *nexmifb* morphants was significantly shorter than that in the control group ($P < 0.05$) (Figures 3(a) and 3(b)).

## Knockdown of nexmifb affected the development of spinal motor neurons

We investigated the function of *nexmifb* in zebrafish embryonic development by observing the morphology of PMNs in Tg (*mnx1*: GFP)$^{ml2}$ transgenic zebrafish line by confocal microscopy between control and *nexmifb* morphants. We found knockdown of *nexmifb* caused obvious developmental defects in spinal motor neurons at 72 hpf. Firstly, knockdown of *nexmifb* led to the loss of spinal motor neurons (Figure 4(a)). We divided defective zebrafish embryos into three groups according to the percentage of motor neurons lost: severe group: loss of > 80% of motor neurons; moderate group: loss of 20%–80% of motor neurons; and normal group: loss of < 20% of motor neurons. Results showed that 4.2% of the control group had moderate defects and 95.8% were normal. However, 24.3% of the *nexmifb* morphants were normal, 32.2% had moderate defects, and 43.5% had severe defects (Figure 4(b)). To explore whether the loss of motor neurons was caused by apoptosis, the TUNEL BrightRed Apoptosis Detection Kit was used. We found there was almost no apoptotic signal in the control group. Although the *nexmifb* morphants showed apoptotic signals, they were not colocated with GFP-labeled motor

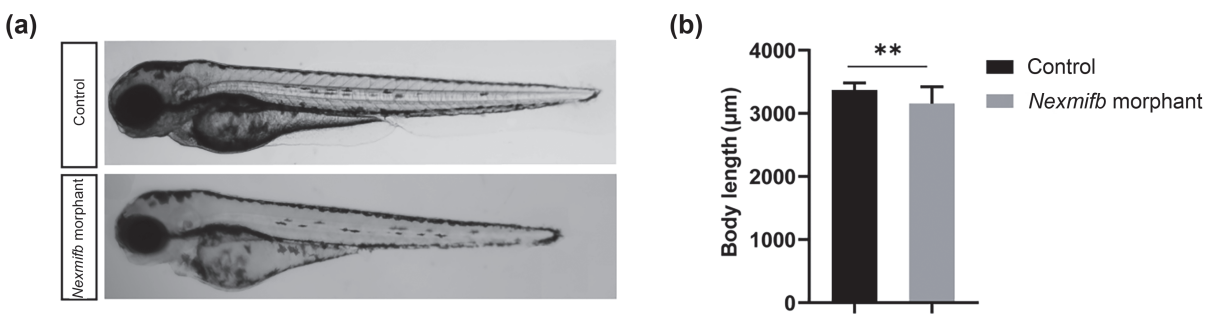


**Figure 3:** Knockdown of *nexmifb* decrease the body length of zebrafish ((a) The body of zebrafish between control and *nexmifb* morphants in open field; (b) Graph of body length in zebrafish at 72 hpf between control and *nexmifb* morphants; $^{**}P < 0.01$).

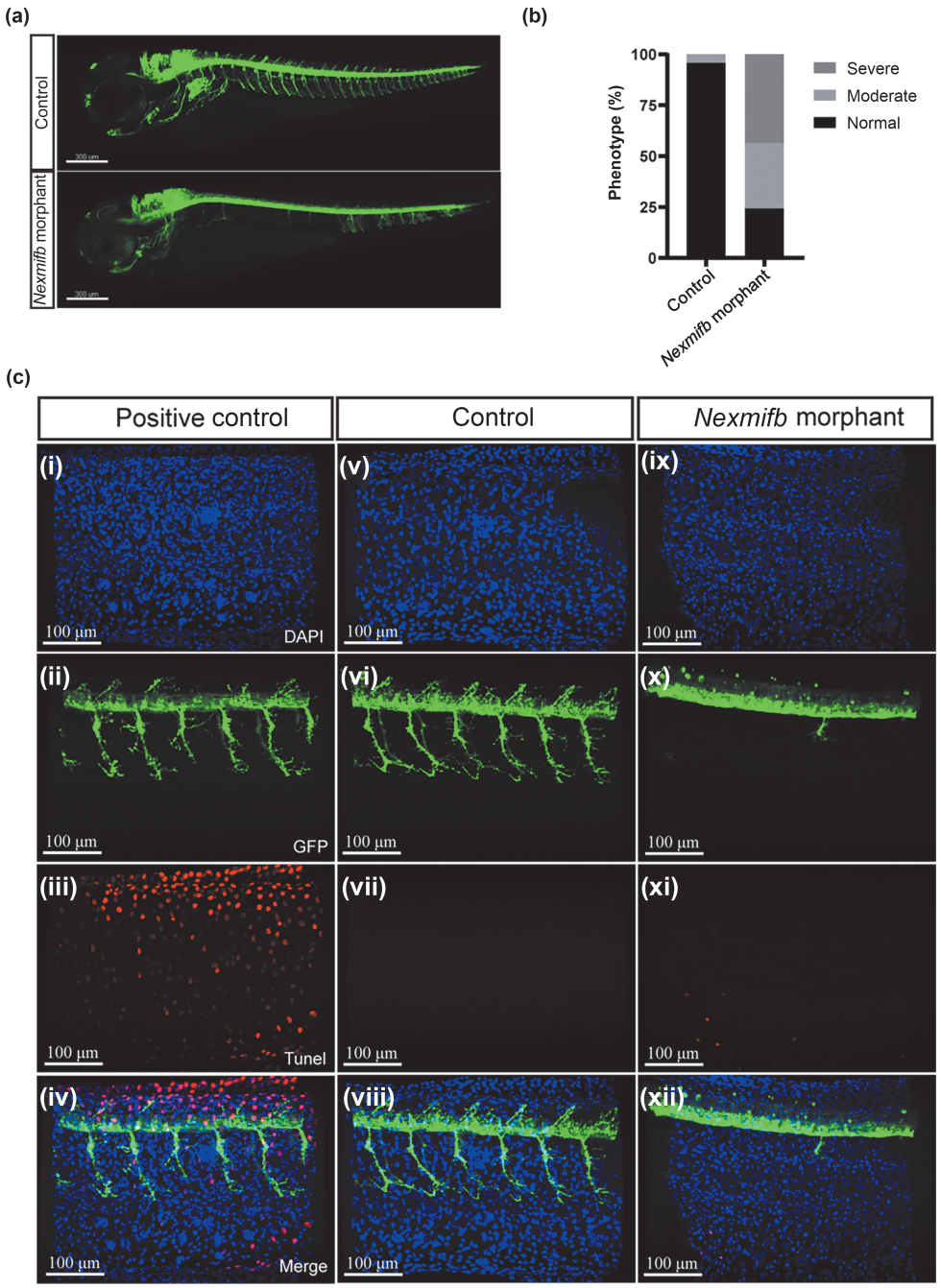


**Figure 4:** Knockdown of *nexmifb* led to the loss of spinal motor neurons. ((a) Confocal imaging of whole fish in controls and *nexmifb* morphants at 72 hpf; (b) Percentage of severe, moderate, and normal group between controls ($n = 194$) and *nexmifb* morphants ($n = 225$); (c) Apoptosis detection between controls and *nexmifb* morphants).

(i), (v), and (ix) Nuclear staining by DAPI among positive control, control, and *nexmifb* morphants in zebrafish; (ii), (vi), and (x) Confocal imaging of GFP-labeled PMNs among the three groups; (iii), (vii), and (xi) TUNEL signal among the three groups; (iv), (viii), and (xii) Merging of DAPI, GFP, and TUNEL staining.

neurons (Figure 4(c)).

Secondly, we also found that some motor neurons may have no loss of motor neurons, but the morphology of CaPs was abnormal. CaP axons were shorter and could not reach the ventral musculature (Figure 5(a)), which indicated significant developmental retardation in the *nexmifb* morphants. Statistical analysis showed that, the branches were disordered, the number of branches per mm of CaP was $77 \pm 12$ in *nexmifb* morphants,

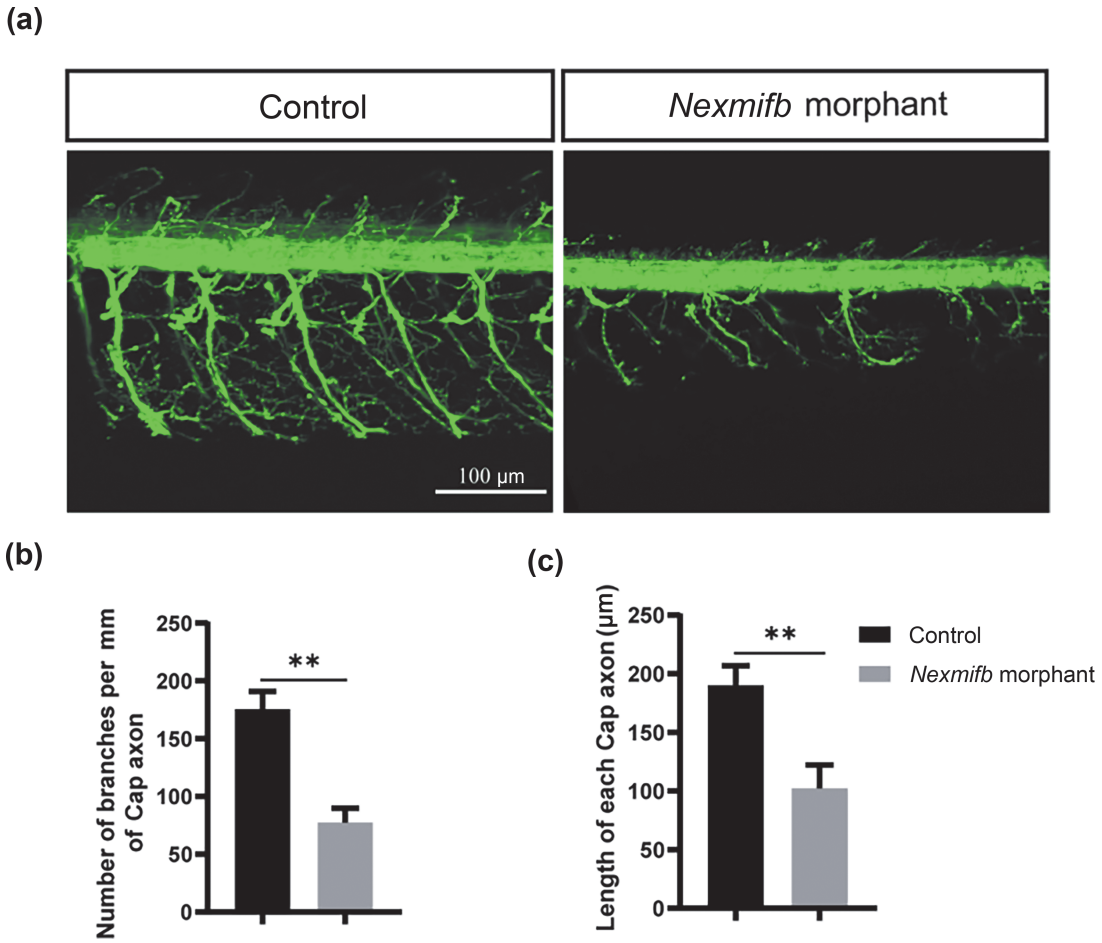


**Figure 5:** Knockdown of *nexmifb* led to the defect of morphogenesis of PMNs ((a) Confocal imaging of PMNs in controls and *nexmifb* morphants at 72 hpf; (b) Number of branches per mm of CaP axon between controls ($n = 17$) and nexmifb morphants ($n = 23$); (c) Length of CaP axons between two groups ($n = 20, 27$, respectively); $^{**}P < 0.01$).

compared with 175 ± 15 in the controls ($P < 0.05$) (Figure 5(b)). The length of CaPs was shorter than that of the controls (190.1 ± 16.7 μm *vs*. 102.2 ± 20.1 μm) ($P < 0.05$) (Figure 5(c)).

## Transcriptomic profiling of nexmifb morphants and control zebrafish

To elucidate the mechanisms underlying the effects of *nexmifb* on motor neuron development, we extracted RNA from control, *nexmifb* morphants and *nexmifa* morphants at 72 hpf and performed RNA-Seq. There were 4119 different expression genes (DEGs) between the control and *nexmifb* morphants (Figure 6(a)). Many DEGs were related to the CNS and can be classified into axon guidance, synapses and so on (Figure 6(b)). Because of knockdown of *nexmifb* can result in a similar abnormal phenotype to that of *nexmifa* morphants; therefore, we investigated whether there was the same mechanism of morphogenesis regulation during spinal motor neuron development between *nexmifb* and *nexmifa*. We compared the DEGs between the control and *nexmifa* morphants and between the control and *nexmifb* morphants, then found there were different and common DEGs between them. There were 1665 common DEGs, among which, 825 were common down-regulated and 288 were common up-regulated (Figure 6(c)). Among the common down-regulated DEGs, 21 were enriched in the axon guidance pathway (Figure 6(d)), which was related to the abnormal phenotype induced by *nexmif* deficiency. These results indicate that *nexmifa* and *nexmifb* may have similar mechanisms in regulation the development of spinal motor neuron. Using the change fold as our criterion, we used qRT-PCR to verify the

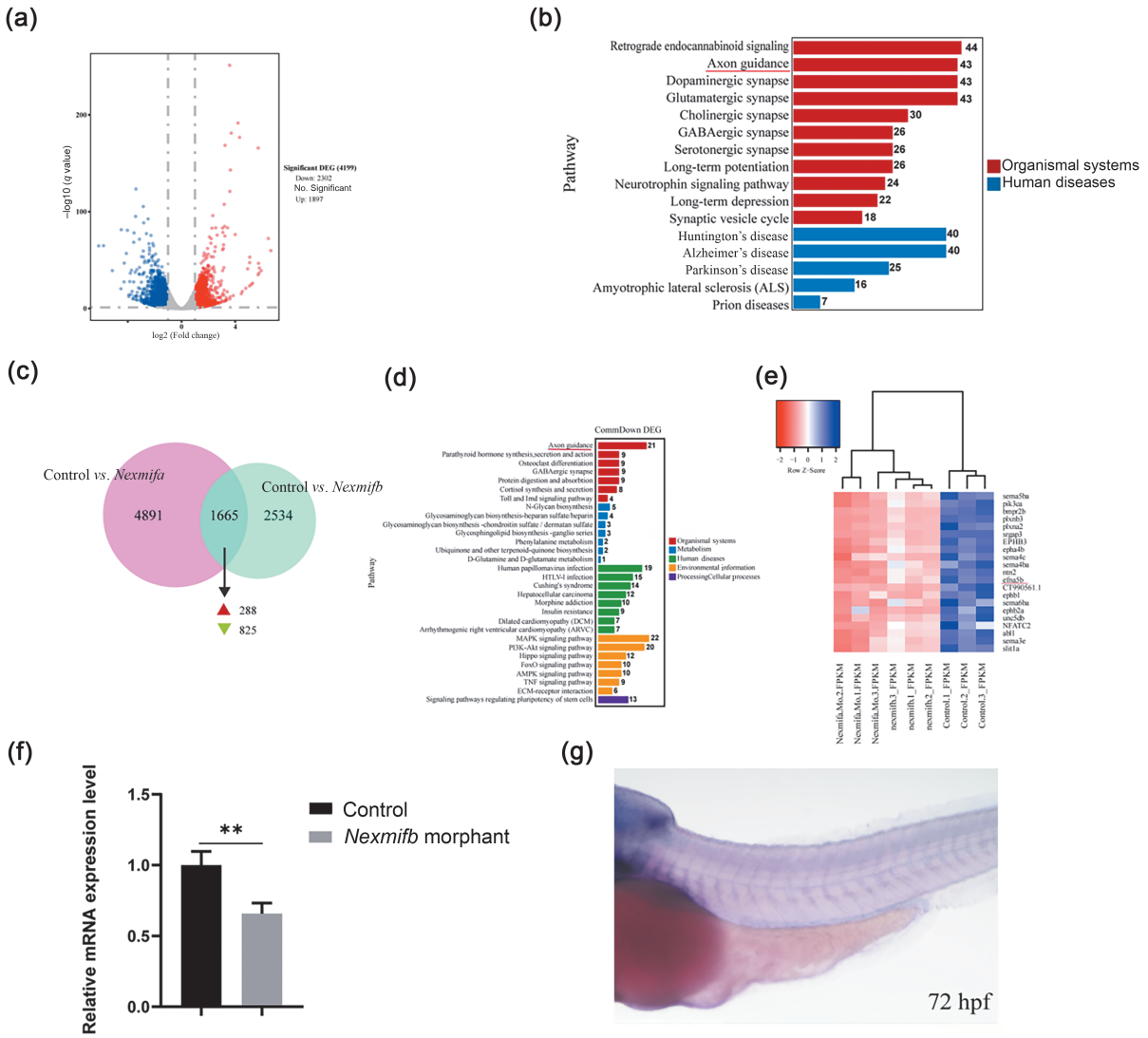


**Figure 6:** RNA-Seq of control, *nexmifb* morphants and *nexmifa* morphants ((a) Volcano map showing DEGs in control and *nexmifb* morphants. Red and blue spots represent up-regulated and down-regulated genes, respectively; (b) KEGG enrichment pathway annotation of DEGs in control and *nexmifb* morphants related to CNS according to organismal systems and human diseases; (c) Venn map showing DEGs in control *vs.* *nexmifb* morphants, and control *vs.* *nexmifa* morphants; (d) KEGG pathway annotation of common down-regulated DEGs in control *vs.* *nexmifb* morphants, and control *vs.* *nexmifa* morphants; (e) Heatmap of 20 common down-regulated DEGs in control *vs.* *nexmifb* morphants, and control *vs.* *nexmifa* morphants involved in the axon guidance pathway; (f) Expression of efna5b in control *vs.* *nexmifb* morphants by qRT-PCR; (g) Expression of efna5b in zebrafish at 72 hpf by WISH; $^{**}P < 0.01$).

expression of *efna5b*, which showed the greatest change among the 21 common down-regulated DEGs in *nexmifb* morphants compared to controls at 72 hpf. (Figure 6(e) and 6(f)). We also found *efna5b* was expressed in spinal cord of zebrafish by WISH (Figure 6(g)).

## *Efna5b overexpression rescued motor neuron defects in nexmifb-deficient embryos*

To investigate the molecular mechanism by which *nexmifb* regulates spinal motor neuron development in zebrafish, we selected *efna5b*, which had the largest fold change. Then we synthesized *efna5b* mRNA *in vitro* and coinjected them with *nexmifb* MOs into the yolk of one-cell embryos to explore whether *nexmifb* regulates the development of spinal motor neurons through the down-regulate expression of *efna5b*. We observed at 72 hpf, 6.9% of the control embryos had moderate defects and 93.1% were normal, 39.2% of the *nexmifb* morphants had severe defects, 32.2% had moderate

defects, and 28.6% were normal. After overexpression of *efna5b*, normal were increased to 68.5%, severe and moderate defects were decreased to 20.8% and 10.7%, respectively (Figure 7(a) and 7(b)).

The abnormal of CaPs length and the number of branches were also rescued (Figure 7(c) and 7(d)). The lengths of CaPs in the *nexmifb* morphants was 121.4 ± 27.3 μm, which was significantly less than that in the control group (202.3 ± 18.9 μm). However, the lengths of CaPs dramatically increased to 183.0 ± 33.5 μm when the morphants were coinjected with *efna5b* mRNA (Figure 7(c)). The number of branches per mm of CaPs in the *nexmifb* morphants was less than that in the control group (85 ± 20 *vs*. 181 ± 9). However, the number of branches dramatically increased to 120 ± 28 when the morphants were coinjected with *efna5b* mRNA (Figure 7(d)).

## Discussion

Previous studies have indicated that NEXMIF plays an important role in the development of CNS, especially in the brain. However, the relationship between *nexmifb* and the spinal cord remains unclear. In this study, we provide new insights into the role of *nexmifb* in spinal motor neuron development by examining the expression of *nexmifb*, established *nexmifb* knockdown model, which may provide therapeutic targets for motor neuron diseases.

WISH and RT-PCR indicated that *nexmifb* was mainly expressed in brain and spinal motor neurons which indicates that *nexmifb* may regulate the development of motor neurons directly. Therefore, we established a *nexmifb* knockdown model to characterize PMN morphology. *nexmif* has two paralogs in zebrafish. In order to illustrates whether there was a compensatory effect between *nexmifa* and *nexmifb*, we detected expression of *nexmifb* in *nexmifa* morphants and expression of *nexmifa* in *nexmifb* morphants by qRT-PCR and finally draw a conclusion that there was no compensation

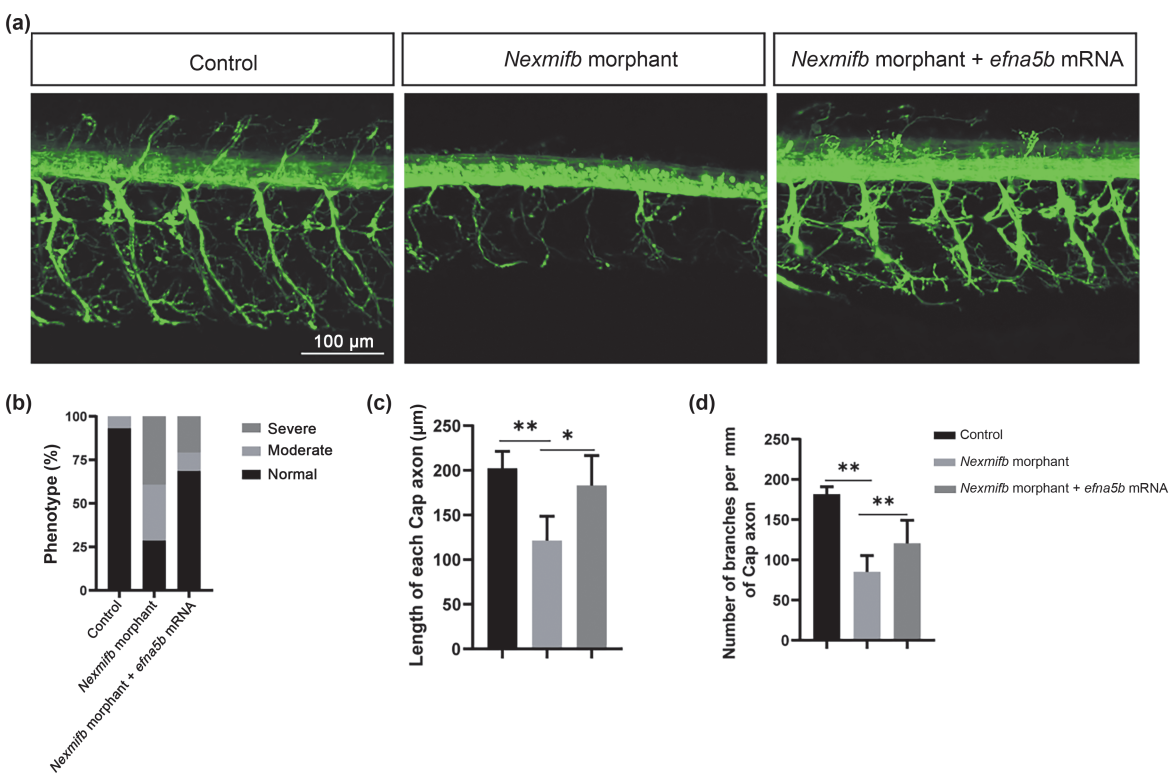


**Figure 7:** *efna5b* overexpression rescued the abnormal PMNs phenotype caused by the decrease of *nexmifb* ((a) Confocal imaging of PMNs in the control, *nexmifb* morphant and *nexmifb* morphant + *efna5b* mRNA; (b) Percentage of severe, moderate, and normal defect embryos among the three groups ($n$ = 188, 225, 230, respectively); (c) The length of CaPs axons among the three groups ($n$ = 18, 25, 27, respectively); (d) The number of branches per mm of CaPs among the three groups ($n$ = 18, 26, 29, respectively); *$P < 0.05$; **$P < 0.01$).

between the two paralogous genes.

We used confocal laser imaging to investigate the requirement of *nexmifb* in the formation of PMNs. During PMNs development, the three kinds of motor neurons extend their axons along stereotypical pathways and branches invade the myotome to form neuromuscular synapses. At 48 hpf, the axons of CaP extend to the middle of the segment, forming a collateral at the horizontal septum. At the ventral edge of the musculature, each axon turns dorsally and laterally grows along the rostral myoseptum[13]. When the embryo develops to 72 hpf, the formation of branches increases and they invade the myotome to form neuromuscular synapses[18,19]. Our data show that knockdown of *nexmifb* results in "CaPs and/or MiPs loss" as well as abnormal PMNs morphology. These results suggest that *nexmifb* is pivotal for the development of PMNs.

The types of cell death mainly include apoptosis, necrosis, and autophagy. RNA-Seq showed some DEGs associated with apoptosis between control and *nexmifb* morphants (NCBI BioProject PRJNA1157466); therefore, we speculated whether the loss of spinal motor neurons was caused by apoptosis. We found the number of apoptotic cells in *nexmifb* morphants, but the TUNEL signal was not co-located with motor neurons. These results suggest that the knockdown of *nexmifb* may lead to apoptosis of other cells rather than spinal motor neurons and that the loss of motor neurons may result from other modes of death. However, maybe there is another explanation that the "loss of motor neurons" is just the lack of axonal projection rather than the loss of cell bodies and axonal projection due to apoptosis, and all these require further investigation.

The development of spinal cord motor neurons begins at the embryonic stage and continues to the early postnatal stage. During this period, motor neurons are regulated by a variety of genes, such as transcription factors, channels, receptors, collagen, kinases, chromatin regulatory genes, etc[20]. For example, *insm1a* regulates spinal motor neuron development through *olig2* and *nkx6.1*[21]. Although its expression was weak in the spinal cord, deficiency of *sema6D* induced by injection of *sema6D*-MOs caused dramatic developmental defects in PMNs, such as decreased length of CaPs, decreased number of branches, and the misdirected axonal trajectories[22]. Our RNA-Seq data showed that there were many DEGs between the controls and *nexmifb* morphants involved in neural development, synapses and axon guidance. In addition, compared with the RNA-Seq data between the controls and *nexmifa* morphants, there were many common down-regulated DEGs including *efna5b* which enriched in axon guidance pathway according to KEGG.

*Efna5b*, also known as *ephrin-A5b*, belongs to the Ephrins/Eph family of axon guidance molecules and represents a crucial class of axon guidance molecules[23,24]. The Ephrins/Eph family exhibits bidirectional regulatory functions; for instance, it can act as a ligand for Eph receptors and also function as a receptor for Eph ligands[25]. In Caenorhabditis elegans, ephrin EFN-4 promotes primary neurite outgrowth in AIY interneurons and class D motor neurons[26]. Increased expression of ephrinA5 in the retina enhances TrkB signaling, thereby promoting axon branching[27]. Poopalasundaram et al.[25] suggested that ephrinA6 is involved in retinal axon guidance and branching functions. They found that downregulation of ephrinA6 significantly reduces BDNF-induced axon branching in the chick retina and that ephrinA is critical for p75NTR-dependent axon guidance repulsion as well as TrkB-mediated branching. Flanagan and Vanderhaeghen[28] discovered that, in cultured retinal ganglion cells *in vitro*, ephrin A5 induces growth cone collapse, whereas in *in vivo* experiments, ephrin A5 promotes axon growth.

In our study, *efna5b* was expressed in the spinal cord, and its expression was dramatically down-regulated in *nexmifb* knockdown embryos compared with controls. Overexpression of *efna5b* partly rescued the abnormal PMNs phenotype. These data showed that *nexmifb* can affect spinal PMNs development by regulating the expression of *efna5b*.

In summary, our study first demonstrated that *nexmifb* was not only located in the brain but also in the spinal motor neurons. It plays a crucial role during motor neuron development, at least in part, through the down-regulation of *efna5b*. This work will deepen a comprehensive understanding of *nexmifb* functions and provide potential therapeutic targets for motor neuron disease.

## Acknowledgments

Not applicable.

## Authors' contributions

Mei Sun: methodology, investigation, visualization, writing- original draft preparation, writing-review & editing. Zirui Zhou: methodology, investigation, writing-review & editing. Jingwen Ma: visualization. Lingling Li: investigation. Youjia Wu: validation. Guihai Suo: conceptualization, supervision, project administration. Yuqin Zheng: conceptualization, supervision, project administration, funding acquisition. All authors have read and agreed to the published version of the manuscript.

## Fundings

This research was supported by Nantong Municipal Health Commission (MS2025024), Nantong Municipal Health Commission (MS2024004), Jiangsu Medical Association Pediatric Special Program for Medical Research Projects (SYH-32034-0151, 2025028) and the Open Project program of Guangxi Key Laboratory of Children's Disease Research in 2024 (GXCDR202403).

## Ethics approval and consent to participate

All animal experimentation was carried out by the NIH Guidelines for the Care and Use of Laboratory Animals, (accessed on 25 June 2022) and ethically approved by the Administration Committee of Experimental Animals, Jiangsu Province, China (approval ID: 20150305-029). Zebrafish were euthanized by immersion in 300 mg/L tricaine at 4 °C for 10 min. All experiments were performed under ARRIVE guidelines. All participants provided written informed consent for an interview, as well as follow-up interviews.

## Disclosure of artificial intelligence (AI) use

All authors declare that no AI was used in the writing and publication of this article.

## Competing interests

The authors declare no conflicts of interest.

## Consent for publication

The authors give the consent for the publication of identifiable details, which can include figures and data details within the text to be published by *Translational Neurology and Neurosurgery*.

## Data availability statement

Ranscriptomic datasets presented in this study can be found in online repositories. The names of the repository/repositories and accession number(s) can be found below: NCBI BioProject PRJNA1157466. Other data is provided within the manuscript.

## References

1. Cantagrel V, Lossi AM, Boulanger S, et al. Disruption of a new x linked gene highly expressed in brain in a family with two mentally retarded males. *J Med Genet*. 2004;41(10):736-742.
2. Wang L, Li Z, Song X, et al. Bioinformatic analysis of genes and micrornas associated with atrioventricular septal defect in down syndrome patients. *Int Heart J*. 2016;57(4):490-495.
3. Stekelenburg C, Blouin JL, Santoni F, et al. Loss of nexmif results in the expression of phenotypic variability and loss of genomic integrity. *Sci Rep*. 2022;12(1):13815.
4. Cantagrel V, Haddad MR, Ciofi P, et al. Spatiotemporal expression in mouse brain of kiaa2022, a gene disrupted in two patients with severe mental retardation. *Gene Expr Patterns*. 2009;9(6):423-429.
5. Zhong L, Liu C, Lin L. Infantile spasms caused by nexmif mutation: a case report and literature review. *Appl Neuropsychol Child*. 2023;12(4):380-385.
6. Wang L, Huang Y, Liu X. Nexmif pathogenic variant in a female child with epilepsy and multiple organ failure: a case report. *Transl Pediatr*. 2023;12(6):1278-1287.
7. Langley E, Farach LS, Koenig MK, et al. Nexmif pathogenic variants in individuals of korean, vietnamese, and mexican descent. *Am J Med Genet A*. 2022;188(6):1688-1692.
8. Gilbert J, Man HY. The x-linked autism protein kiaa2022/kidlia regulates neurite outgrowth via n-cadherin and delta-catenin signaling. *Eneuro*. 2016;3(5):ENEURO.0238-16.2016.
9. Magome T, Hattori T, Taniguchi M, et al. Xlmr protein related to neurite extension (xpn/kiaa2022) regulates cell-cell and cell-matrix adhesion and migration. *Neurochem Int*. 2013;63(6):561-569.
10. Gilbert J, O'Connor M, Templet S, et al. Nexmif/kidlia knock-out mouse demonstrates autism-like behaviors, memory deficits, and impairments in synapse formation

and function. *J Neurosci*. 2020;40(1):237-254.
11. Purifoy EJ, Mruk K. Differential roles of diet on development and spinal cord regeneration in larval zebrafish. *Zebrafish*. 2024;21(2):214-222.
12. Myers PZ. Spinal motoneurons of the larval zebrafish. *J Comp Neurol*. 1985;236(4):555-561.
13. Myers PZ, Eisen JS, Westerfield M. Development and axonal outgrowth of identified motoneurons in the zebrafish. *J Neurosci*. 1986;6(8):2278-2289.
14. Westerfield M, McMurray JV, Eisen JS. Identified motoneurons and their innervation of axial muscles in the zebrafish. *J Neurosci*. 1986;6(8):2267-2277.
15. Eisen JS, Myers PZ, Westerfield M. Pathway selection by growth cones of identified motoneurones in live zebra fish embryos. *Nature*. 1986;320(6059):269-271.
16. Beattie CE, Granato M, Kuwada JY. Cellular, genetic and molecular mechanisms of axonal guidance in the zebrafish. *Results Probl Cell Differ*. 2002;40:252-269.
17. Zheng YQ, Suo GH, Liu D, et al. Nexmifa regulates axon morphogenesis in motor neurons in zebrafish. *Front Mol Neurosci*. 2022;15:848257.
18. Liu DW, Westerfield M. The formation of terminal fields in the absence of competitive interactions among primary motoneurons in the zebrafish. *J Neurosci*. 1990;10(12):3947-3959.
19. Downes GB, Granato M. Acetylcholinesterase function is dispensable for sensory neurite growth but is critical for neuromuscular synapse stability. *Dev Biol*. 2004;270(1):232-245.
20. Catela C, Kratsios P. Transcriptional mechanisms of motor neuron development in vertebrates and invertebrates. *Dev Biol*. 2021;475:193-204.
21. Gong J, Wang X, Zhu C, et al. Insm1a regulates motor neuron development in zebrafish. *Front Mol Neurosci*. 2017;10:274.
22. Sheng J, Xu J, Geng K, et al. Sema6d regulates zebrafish vascular patterning and motor neuronal axon growth in spinal cord. *Front Mol Neurosci*. 2022;15:854556.
23. Cayuso J, Xu Q, Wilkinson DG. Mechanisms of boundary formation by eph receptor and ephrin signaling. *Dev Biol*. 2015;401(1):122-131.
24. Lisabeth EM, Falivelli G, Pasquale EB. Eph receptor signaling and ephrins. *Cold Spring Harb Perspect Biol*. 2013;5(9):a009159.
25. Poopalasundaram S, Marler KJ, Drescher U. Ephrina6 on chick retinal axons is a key component for p75(ntr)-dependent axon repulsion and trkb-dependent axon branching. *Mol Cell Neurosci*. 2011;47(2):131-136.
26. Schwieterman AA, Steves AN, Yee V, et al. The caenorhabditis elegans ephrin efn-4 functions non-cell autonomously with heparan sulfate proteoglycans to promote axon outgrowth and branching. *Genetics*. 2016;202(2):639-660.
27. Marler KJ, Becker-Barroso E, Martinez A, et al. A trkb/ephrina interaction controls retinal axon branching and synaptogenesis. *J Neurosci*. 2008;28(48):12700-12712.
28. Flanagan JG, Vanderhaeghen P. The ephrins and eph receptors in neural development. *Annu Rev Neurosci*. 1998;21:309-345.